Icarus 204 (2009) 183–193

Contents lists available at ScienceDirect

Icarus

journal homepage: www.elsevier.com/locate/icarus

On the composition and differentiation of Ceres

Mikhail Yu. Zolotov *

School of Earth and Space Exploration, Arizona State University, Tempe, AZ 85287-1404, USA

ARTICLE INFO

Article history:
Received 8 October 2008
Revised 7 June 2009
Accepted 12 June 2009
Available online 21 June 2009

Keywords:
Asteroid Ceres
Interiors
Geophysics
Mineralogy
Cosmochemistry

ABSTRACT

The dwarf planet Ceres has a density of 2040–2250 kg m^{-3}, and a dark non-icy surface with signs of hydrated minerals. As opposed to a differentiated internal structure with a nonporous rocky core and a water mantle, there are arguments for undifferentiated porous interior structure. Ceres' mass and dimensions are uncertain and do not exclude undifferentiated interior even if hydrostatic equilibrium is attained. The rocky surface may be inconsistent with a large-scale water–rock differentiation. A differentiated structure with a thick water mantle below a rocky crust is gravitationally unstable and an overturn would have led to abundant surface salt deposits, which are not observed. A formation of hydrated surface minerals caused by internal heating implies a major density increase through devolatilization of the interior. A later accumulation of hydrated materials is inconsistent with anhydrous surfaces of many asteroids and with a low rate of the cosmic dust deposition in the inner Solar System. Ceres' internal pressures (<140–200 MPa) are insufficient to significantly reduce porosity of chondritic materials and there is no need for abundant water phases to be present to account for the bulk density. Having the porosity of ordinary chondrites (~10%), Ceres can consist of rocks with the grain density of pervasively hydrated CI carbonaceous chondrites. However, additional low-density phases (e.g., water ice) require to be present in the body with the grain density of CM chondrites. The likely low-density mineralogy of the interior implies Ceres' accretion from pervasively aqueously altered carbonaceous planetesimals depleted in short-lived radionuclide ^{26}Al. Abundant water ice may not have accreted. Limited heat sources after accretion may not have caused major mineral dehydration leading to formation of water mantle. These inferences can be tested with the Dawn spacecraft in 2015.

1. Introduction

Dwarf planet Ceres is the largest body in the asteroid belt with a diameter of ~950 km and a density of ~2040–2250 kg m^{-3} (Thomas et al., 2005; Carry et al., 2008). This density implies that Ceres contains a significant fraction of low-density compounds. These species can be presented by hydrated and OH-bearing minerals (phyllosilicates, salts, hydroxides), ices (e.g. McCord and Sotin, 2005), clathrate hydrates and organic compounds.

Although there are not good spectral analogs of the Ceres' surface among Earth's, lunar and meteoritic (e.g., Jones et al., 1990) samples, Ceres' reflectance spectra in near- and mid-infrared do not contradict with a volatile-bearing interior. Despite a similarity of Ceres' spectra with that of thermally metamorphosed carbonaceous chondrites (Hiroi et al., 1995), some differences are notable (Sato et al., 1997). Ceres has higher albedo (~0.08) compared to that of carbonaceous chondrites (0.03–0.05) and the difference can be attributed to a larger fraction of high-albedo phases on the planet's surface (McCord and Sotin, 2005).

Ceres' reflectance spectra have a broad absorption feature near 3 μm that probably reflects water of hydration and structural hydroxyl (Lebofsky, 1978; Lebofsky et al., 1981; Feierberg et al., 1981; Jones et al., 1990). Ceres' 3 μm band can represent abundant phyllosilicates (e.g., Lebofsky, 1978), but it is weaker than that in pervasively aqueously altered CI and CM chondrites (Miyamoto and Zolensky, 1992). The nature of absorption near 3.05–3.07 μm, initially attributed to a thin H_2O frost layer (Lebofsky et al., 1981; Jones et al., 1990), remains uncertain, and several volatile-bearing phases have been considered: ammonium-bearing saponite (King et al., 1992), ion-irradiated asphaltites with traces of water ice (Vernazza et al., 2005), a mixture of carbonates and Fe-rich phyllosilicate cronstedtite (Rivkin et al., 2006) and a mixture of brucite ($Mg(OH)_2$) with Mg carbonates (Milliken and Rivkin, 2009). Rivkin et al. (2006) also showed that a carbonate–cronstedtite mixture provides better fit for the mid-infrared (5–12 μm) Ceres' spectrum than NH_4-bearing phyllosilicates. The brucite–carbonate (plus cronstedtite and magnetite?), assemblage looks as a reliable interpretation of Ceres' spectra in ~1–14 μm range (Milliken and Rivkin, 2009). Note that thermal emission spectra of Ceres' surface also indicate a presence of forsteritic (Mg-rich) olivine (Witteborn et al., 2000), which may indicate incomplete aqueous alteration of surface materials.

* Fax: +1 480 965 8102.
E-mail address: zolotov@asu.edu.

0019-1035/$ - see front matter © 2009 Elsevier Inc. All rights reserved.
doi:10.1016/j.icarus.2009.06.011

The lack of firm identification of surface water ice agrees with its instability at the current maximum surfaces temperature of ~235 K (Fanale and Salvail, 1989). Microwave observations of Ceres are consistent with a 3-cm-thick surface layer of dry clay (Webster et al., 1988). The notable absorption at 3.3–3.4 μm could be due to aromatic hydrocarbons (Moroz et al., 1998; Rivkin et al., 2006), consistent with Ceres' low albedo. All these data suggest that the dwarf planet contains H_2O- and/or OH-bearing phases and organic compounds that are typically present in carbonaceous chondrites. Whether hydrated and organic minerals are exclusively abundant in surface materials or represent Ceres' interior is not known.

Theoretical assessments have been used to evaluate several alternative models for the Ceres' internal structure (McCord and Sotin, 2005), to face the arrival of the Dawn spacecraft in 2015 (Russell et al., 2007). All the models considered by McCord and Sotin (2005) require the presence between 17 and 27 mass% of water (ice and/or liquid) in nonporous interior. This paper presents arguments for a hydrated porous interior structure without abundant ice.

2. A case for hydrated interior without icy mantle

According to one of the end-member models of McCord and Sotin (2005), Ceres may consist of a mixture of hydrated minerals with water phases (ice + liquid?) and is not differentiated. Although McCord and Sotin (2005) preferred a rock-ice differentiated interior with a 40–105 km water layer atop a rocky core (cf. Castillo-Rogez and McCord, 2009), a compositionally homogeneous structure with a moderate density gradient remains a possibility.

Current estimates of Ceres' second degree gravitational moment (J_2) are based on telescopic data on the body's dimensions, mass, spin period and an assumption that rotational hydrostatic equilibrium is attained (McCord and Sotin, 2005). A homogeneous Ceres would have $J_2 = (29.9–31.7) \times 10^{-3}$ (depending on data used, see Section 3.2) while differentiated internal structures would have J_2 values from $\sim 16 \times 10^{-3}$ to $\sim 24 \times 10^{-3}$ (McCord and Sotin, 2005). Based on HST observations, Thomas et al. (2005) reported density of ~2077 kg m^{-3} and ~32.6 km difference between equatorial and polar radiuses (flattening). These values and the corresponding $J_2 = 21.7 \times 10^{-3}$ imply a differentiated interior structure. However, Keck telescopic observations by Carry et al. (2008) lead to density of ~2206 kg m^{-3}, the flattening of ~35.3 km, and $J_2 = 26.7 \times 10^{-3}$. Although Carry et al. (2008) argued for a differentiated Ceres, their data suggest less differentiation, and an undifferentiated case is possible (Fig. 1).

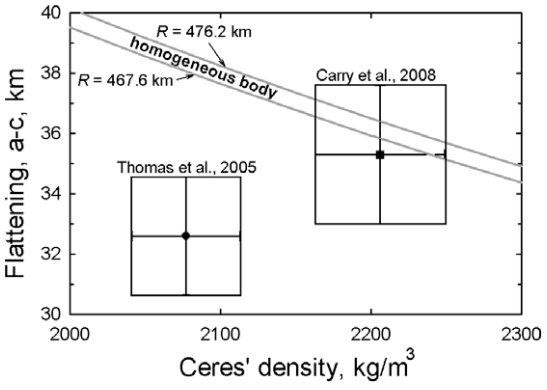

Fig. 1. Recent data on Ceres' shape and density. The *Y*-axis shows the difference between equatorial (a) and polar (c) radius. The gray curves represent modeled shape-density relations (Eqs. (A4)–(A7) in Appendix A) for a homogeneous body with rotation period of 9.074 h for equivalent radius ($\sqrt[3]{aac}$) from Thomas et al. (2005) (upper curve) and Carry et al. (2008) (lower curve). The plot shows that data of Carry et al. (2008) are consistent with interior structure with uniform density distribution or with structure with a moderate density gradient.

Ceres may not be at the state of complete rotational hydrostatic equilibrium and the evaluated J_2 numbers may not represent the interior structure. Venus, Mars, Mercury and the Moon deviate from the ideal hydrostatic equilibrium. Even not every large low-density icy body attains the equilibrium: Titan is nearly hydrostatic (Rappaport et al., 2008) but Callisto is not (McKinnon, 1997). The relative small size of Ceres compared to these icy satellites and low temperatures in the interior (<350–400 K, McCord and Sotin, 2005) do not favor the equilibration. Furthermore, the achievement of hydrostatic equilibrium is less favorable if Ceres has no low-viscosity water mantle. An early cessation of interior processes driven by decay of ^{26}Al (McCord and Sotin, 2005; Castillo-Rogez and McCord, 2009) and only mild warming by long-lived ^{40}K and ^{232}Th (McCord and Sotin, 2005) could have limited changes in the body's shape throughout history. Ceres' accretion of planetesimals with decayed ^{26}Al, as discussed below, would have also limited thermal processes and shape adjustments even at early stages of history.

Physical characteristics of Ceres' surface do not indicate an existence of interior water (ice + liquid?) layer. Possible large impact features (Carry et al., 2008) do not reveal signs of exposed ice, and potentially large altitude variations (<18 km, Carry et al., 2008; Li et al., 2006) and surface roughness at the scale of 10–10^4 m (Li et al., 2006) may imply a substantial thickness of the rocky layer atop an icy mantle, if it exists. Although a water mantle layer might have formed during the rock–water differentiation, it should be gravitationally unstable below a cold primordial rocky crust (McCord and Sotin, 2005; Castillo-Rogez and McCord, 2009). At least temporal existence of a thick layer of liquid water below the rocky crust makes the overturn likely. Impacts and tectonic movements caused by phase volume changes during differentiation and water–rock reactions (if they occurred on Ceres) could have favored the submergence of rocky crust. The probable formation of uppermost water layer through rock–water differentiation has been demonstrated for icy satellites (e.g., Schubert et al., 1981; McKinnon and Parmentier, 1986; Kirk and Stevenson, 1987). In contrast to icy satellites, Ceres' uppermost water ice layer should have been sublimated (Fanale and Salvail, 1989).

If a primordial rocky shell sunk into water mantle, the origin of present rocky surface with secondary minerals remains to be explained. If a water layer has formed on Ceres, the liquid fraction (an ocean) should have contained solutes leached from rocks and accreted non-water ices. Major solutes could be presented by Na-, Cl-, Ca-, K-, and C-bearing ions and neutral species (see Section 4.2 and Zolotov, 2007). Sulfates may or may not be present depending on the degree of sulfide oxidation in accreted planetesimals and/or in Ceres' interior. If formed, sulfate-rich aqueous fluids could also be rich in Mg, which is consistent with abundant Mg sulfates in CI chondrites (Brearley and Jones, 1998) and supported by models for water–chondrite interaction (see Section 4.2). Accretion of aqueously processed planetesimals similar to CI chondrites would have led to significant amounts of highly soluble Mg sulfates in Ceres' primordial fluids (cf. Kargel, 1991), if they formed. Freezing and then sublimation of the outer water shell would have led to deposition of salts atop the silicate core (i.e. at the Ceres' surface). Chlorides of Na, K and Ca, and sulfates of Mg and Na rather than low-solubility carbonates of Ca, Mg, and Fe could dominate among the surface salts. Even without abundant Mg sulfate, several hundreds of meters of salt deposits could have accumulated atop the rocks, as it was modeled for early Enceladus (Zolotov, 2007). However, this scenario may be inconsistent with very uniform and low surface albedo (e.g., Li et al., 2006; Carry et al., 2008), with signs of

abundant carbonates formed together with phyllosilicates (Rivkin et al., 2006; Rivkin and Volquardsen, 2008) and brucite (Milliken and Rivkin, 2009), and with the lack of spectral signatures of sulfates and chlorides. Although impacts could have mixed surface salts with rocks and partially obliterated the salts, a salt accumulation scenario implies a small amount of precipitated salts from a low-volume water envelope. It is possible that Ceres' water layer could never have formed. If formed, it could be thin and/or deep enough to prevent the gravitational overturn and formation of abundant high-solubility salts at the surface.

A cosmic accumulation of abundant hydrated minerals atop an icy mantle or salt deposits is inconsistent with the absence of such materials on Vesta and many other asteroids with orbital distances of 2–3 AU (Jones et al., 1990; Gaffey et al., 2002), with the ice-bearing surface of Callisto, and with a slow accumulation of cosmic dust on the Moon and other inner Solar System bodies (Peucker-Ehrenbrink and Schmitz, 2001; Yada et al., 2004). It follows that secondary minerals of Ceres' surface could have resulted from *in situ* aqueous alteration and/or represent hydrated planetesimals from which the planet accreted.

Alteration of surface rocks *in situ* does not contradict to the uniform spatial occurrence of spectral features attributed to Fe-phyllosilicates and carbonates that may indicate aqueous precipitation of both minerals (Rivkin and Volquardsen, 2008). However, Ceres' thermal evolution models do not predict ice melting in the uppermost rock layer (McCord and Sotin, 2005; Castillo-Rogez and McCord, 2009), and water boiling and/or freezing near the surface makes pervasive alteration unlikely. It is hard to explain significant heating of surface materials, especially if they are located atop a water layer. The *in situ* alteration of surface rocks would suggest significant heating and possible devolatilization of Ceres' interior powered by the decay of ^{26}Al (cf. McCord and Sotin, 2005). Such devolatilization implies significant incense in bulk density that is not consistent with observations. Therefore, Ceres' accretion from low-density hydrated planetesimals and a small amount (if any) of water ice is a preferable pathway.

A low porosity of Ceres suggested in (McCord and Sotin, 2005; Thomas et al., 2005) implies the presence of additional low-density constituents compared to typical chondritic materials. For nonporous Ceres, estimated water ice mass fraction is ~0.16 to ~0.27 for hydrated and anhydrous rocks, respectively (Thomas et al., 2005; McCord and Sotin, 2005). However, the ice fraction would be lower if Ceres' porosity is not negligible and/or additional low-density components are present.

Although Ceres' bulk density is similar to that of CM carbonaceous chondrites (Table 1), Ceres' porosity would have to be larger than that of the CM chondrites, which is not supported by the fact that porosity decreases with pressure. If follows that Ceres' bulk density is not compatible with that of CM chondrites unless additional low-density components are present. However, Ceres' density is compatible with the density and porosity of CI chondrites provided that porosity does not decrease too much with pressure.

Table 1
Ceres' average porosity evaluated from grain densities of suitable chondritic analogs.

	Average grain density (kg m^{-3})	Average bulk density (kg m^{-3})	Average porosity (%)
CM chondrites	2900 ± 80	2250 ± 80	23.1 ± 4.7
CI chondrites	2460 ± 40	1600 ± 30	35
Ceres with bulk density from Thomas et al. (2005)			
CM-like grain density	2900 ± 80	2077 ± 36	28.4 ± 0.8
CI-like grain density	2460 ± 40	2077 ± 36	15.6 ± 0.3
Ceres with bulk density from Carry et al. (2008)			
CM-like grain density	2900 ± 80	2206 ± 43	23.9 ± 0.7
CI-like grain density	2460 ± 40	2206 ± 43	10.3 ± 0.2

Notes: Data for CM and CI carbonaceous chondrites are from Consolmagno et al. (2008). Ceres' porosities are calculated with Eq. (2).

3. Constraints on Ceres' porosity, grain density and gravitational parameters

3.1. Compaction of terrestrial and chondritic analogs

Considering that pressure (P) is the major parameter that controls porosity, the low pressure of 140–200 MPa at Ceres' center (see Section 3.2) implies that some porosity (ω) may exist throughout the interior. This pressure corresponds to that only ~4–8 km below the Earth's surface, and P–ω relations are known for major rock types from nature observations (e.g., Allen and Allen, 2005; Giles, 1997), experiments and theoretical analysis (Handin et al., 1963; Edmond and Paterson, 1972; Wash and Brace, 1984; Scott and Nielsen, 1991; Wong, 1990; Dvorkin et al., 1991; Menéndez et al., 1996). Although deposits with small grain sizes (sands to clays) could become impermeable at $P >$ ~300 MPa (e.g., Wash and Brace, 1984; Yang and Aplin, 2004), they may still comprise significant microporosity due to microcracking.

In terrestrial sedimentary basins, the decrease of porosity with depth (h) can be expressed by empirical equation

$$\omega = \omega_o e^{-ch}, \quad (1)$$

where ω_o stands for porosity at the surface and coefficient c represents a rock type (Allen and Allen, 2005). Fig. 2 illustrates changes in porosity of typical deposits calculated with Eq. (1). Particle grain size and a fraction of clay-size (~1 μm, Meunier, 2005) grains play the major role in the pattern of porosity reduction (Yang and Aplin, 2004). Sands are less compactable than clays and shales, and significant porosity remains in them at Ceres' pressures.

Sandstones are much less compactable than unconsolidated deposits (Wong, 1990; Wong et al., 1997). High porosity of typical sandstones (18 ± 8%) is accounted for by their low density of 2200 ± 230 kg m^{-3} (Johnson and Olhoeft, 1984), which matches Ceres' density from Carry et al. (2008). The presence of cement at grain contacts alleviates the tensile stress concentration and

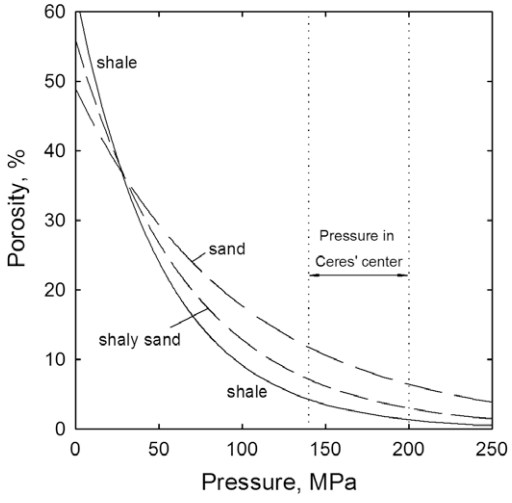

Fig. 2. The compaction of clastic deposits in sedimentary basins on Earth. The curves are calculated with Eq. (1) with coefficients c reported for the North Sea basins (Sclater and Christie, 1980). The values for c are 0.51, 0.39 and 0.27 for shale, shaly sand and sand, respectively. Hydrostatic pressure is calculated for the rock density of 2700 kg m^{-3}. The plot illustrates that clastic rocks in Ceres' center can have porosity of ~2–12%. If grains are cemented, the porosity could be higher than that in sands.

inhibits pore collapse and grain crushing (Dvorkin et al., 1991; Menéndez et al., 1996). Clay particles between mineral grains may play similar role as carbonate cements (Antonellini et al., 1994). In contrast to clays and sands in sedimentary basins, sandstones often demonstrate linear decrease in porosity at $h < 2$–3 km (Allen and Allen, 2005). At $h = 4$–5 km, the sandstones have porosity of 3–18%, and for the majority of data $\omega > 7\%$ (Allen and Allen, 2005; Giles, 1997). Experimental data show that at $P = 300$–800 MPa, sandstones can still preserve a high porosity due to pore space; and at 150 MPa, porosity reduction can be as low as 2–3% (Edmond and Paterson, 1972; Menéndez et al., 1996). In porous sandstones, the transition from brittle faulting to cataclastic flow (when pore space collapses) typically occurs at $P > 100$–150 MPa, and the transition pressure is higher for smaller grains and lower initial porosities (Wong, 1990; Wong et al., 1997).

Density–porosity properties of chondrites, which are classic rocks in which mineral grains are often cemented by secondary minerals, could resemble Earth's sandstones (Consolmagno et al., 1998, 2008). Different classes of chondrite falls have average porosity of ~10% (except CI/CM chondrites with porosity >~20%), and the porosity is not a function of petrographic (metamorphic) grade and shock state (Miyamoto et al., 1982; Corrigan et al., 1997; Consolmagno and Britt, 1998; Consolmagno et al., 2008). In particular, this suggests that mineral dehydration has a little effect on porosity. The lack of clear trends indicates the paucity of large void spaces and implies a common origin of porosity in chondrites. In most chondrite types (except probably CI/CM), microcracks are mainly accountable for total porosity (Consolmagno et al., 2008). Microporosity of ~2% to ~20% also has no correlation with the type of chondrite, and it is much higher than microporosity of typical Earth' rocks (Strait and Consolmagno, 2004). The large contribution of microcrack porosity in chondrites may account for the limited compressibility of their parent asteroids (Consolmagno et al., 2008) and Ceres. In fact, well-studied small asteroids have 20–70% porosity (Britt et al., 2002).

Although stronger impact compaction of Ceres compared to parent bodies of known chondrites may have led to lower porosities, the decrease could not be large. In fact, 9–12% porosity remains in mineral powders even after applying shock pressure of 2.5 GPa (Hirata et al., 1998). A decrease of porosity to ~5% requires $P = 12$–20 GPa. Dissipation of kinetic energy in porous chondritic materials also prevented pressure buildup and limited pore collapse. Therefore, during Ceres' accretion, porosity would have chiefly preserved in target and some projectile materials. As in sandstones and carbonaceous chondrites, Ceres' phyllosilicates, carbonates and other secondary phases could have cemented larger mineral grains and chondrules, and limited compaction. In addition, pore aqueous phase usually limits compaction, and fluids in the target (Ceres) and carbonaceous chondritic projectiles, if they were present, could have limited rock compaction (Consolmagno et al., 1998). Finally, impact reduction of macroporosity could be compensated by the formation of network of microcracks that cut grain boundaries in chondrites (Consolmagno et al., 2008). The impact conversion of macroporosity to microporosity is consistent with a mild and unclear decrease in porosity (down to ~6%) with increasing shock state of chondrites (Consolmagno et al., 2008).

Consolmagno et al. (1998) have stated: "no asteroid is large enough for burial depth to change porosity". Although that statement is based on studied chondritic samples and might be incorrect (Vesta would be nonporous because of ingenious melting), it is likely that microporosity comprises a major fraction of Ceres' porosity (Britt et al., 2002). If Ceres' porosity is not negligible, low-density phases may not be needed to account for the bulk density, as discussed below.

3.2. Evaluations of Ceres' porosity and J_2 gravitational moment

Ceres' bulk porosity (ω_b) can be calculated from bulk density (ρ_b) and grain density (ρ_g) of chondritic analogs via equation

$$\omega_b = [1 - (\rho_b/\rho_g)] \times 100\%, \quad (2)$$

which is widely used to evaluate porosities of asteroids (Britt et al., 2002; Consolmagno et al., 2008). With the use of highly aqueously altered CI and CM chondrites as analogs, calculations with Eq. (2) lead to porosity of ~10% to ~28% (Table 1). Higher porosity corresponds to grain densities of CM chondrites and lower values for Ceres' bulk density. The use of grain densities of other carbonaceous chondrites or ordinary chondrites leads to unrealistically high

Table 2
Modeled geophysical parameters of Ceres that experiences an abrupt collapse of porosity at pressure 60 MPa.

Porosity at $P < 60$ MPa	Porosity at $P > 60$ MPa	r of porosity change (km)	C/MR^2	$J_2 \times 10^3$	Flattening (km)	Grain density (kg m^{-3})	Central pressure (MPa)
Bulk density 2077 kg m^{-3}							
30	0	346	0.372	26.9	35.2	2550	169
30	5	347	0.376	27.5	35.6	2600	164
30	10	350	0.380	28.2	36.1	2660	158
20	0	351	0.382	28.6	36.4	2360	156
20	5	352	0.386	29.2	36.9	2410	151
20	10	354	0.390	30.0	37.4	2470	147
10	0	354	0.391	30.1	37.6	2210	146
10	5	356	0.395	30.9	38.1	2260	141
5	0	356	0.395	30.9	38.1	2140	141
0	0	–	0.4	31.7	38.7	2077	137
Bulk density 2206 kg m^{-3}							
30	0	349	0.372	25.3	32.6	2670	182
30	5	351	0.376	25.9	33.1	2730	176
30	10	353	0.380	26.6	33.5	2800	171
20	0	354	0.382	26.9	33.8	2480	168
20	5	355	0.386	27.6	34.3	2540	163
20	10	357	0.390	28.3	34.8	2610	158
10	0	357	0.391	28.4	34.9	2330	157
10	5	359	0.395	29.1	35.4	2390	153
0	0	–	0.4	29.9	35.9	2206	149

Notes: For bulk density 2077 kg m^{-3}, other used parameters are mass 9.395×10^{20} kg, equivalent radius 476.2 km and equatorial radius 487.3 km (Thomas et al., 2005); for density 2206 kg m^{-3}, the values are 9.43×10^{20} kg, 467.6 km and 479.7 km, respectively (Carry et al., 2008). The body's rotational period is 9.074 h (Carry et al., 2008). Data for zero porosity correspond to a homogeneous body. Calculations are performed with Eqs. (A2)–(A7) in Appendix A.

porosities. However, if Ceres consists of highly hydrated and oxidized materials with the grain density of CI chondrites and has bulk density of ~2200 kg m^{-3} (Carry et al., 2008), the bulk porosity is only ~10%. The ~10% porosity for compacted CI-type materials is realistic because it matches average porosity of many other groups of chondrites (except CI and CM). For example, porosity (≈microporosity) of ordinary chondrite falls is 7.4 ± 5.3% (Consolmagno et al., 2008). Regardless the grain density value used for CI chondritic analogs, these evaluations show that water phases are not required to be present in Ceres' interior. This conclusion is in agreement with the reflectance spectroscopy data and other inferences discussed in Section 2.

Several models can be considered to describe porosity distribution in Ceres' water-less interior. In one end-member case, porosity could be uniformly distributed in homogeneous or compositionally diverse body. For this model, Table 1 gives constraints on porosity for specified bulk and grain densities. In another end-member model, Ceres may have an upper high-porosity layer and a low-porosity core. This hypothetical structure may reflect a mild compaction of sandstone-like carbonaceous chondritic materials and a collapse of pore space at a critical pressure (cf. Wong, 1990). Experimental data on two Earth's sandstones with 35% porosity reveal grain crashing at 42–75 MPa (Wong et al., 1997), and CI-type chondritic materials with similar porosity could sharply decrease their porosity at radial distance 300–400 km from Ceres' center. It is unlikely that the porosity of CI-type materials (35% for Orgueil, Consolmagno et al., 2008; ~40% for ungrouped Tagish Lake carbonaceous chondrite, Brown et al., 2001) will not change at Ceres' pressures. However, pore collapse and grain crushing below a depth of critical pressure should not eliminate the macroporosity (Wong et al., 1997); and microporosity may increase due to grain crashing (Menéndez et al., 1996).

Even for compositionally homogeneous interior, an abrupt collapse of porosity accounts for geophysical parameters that

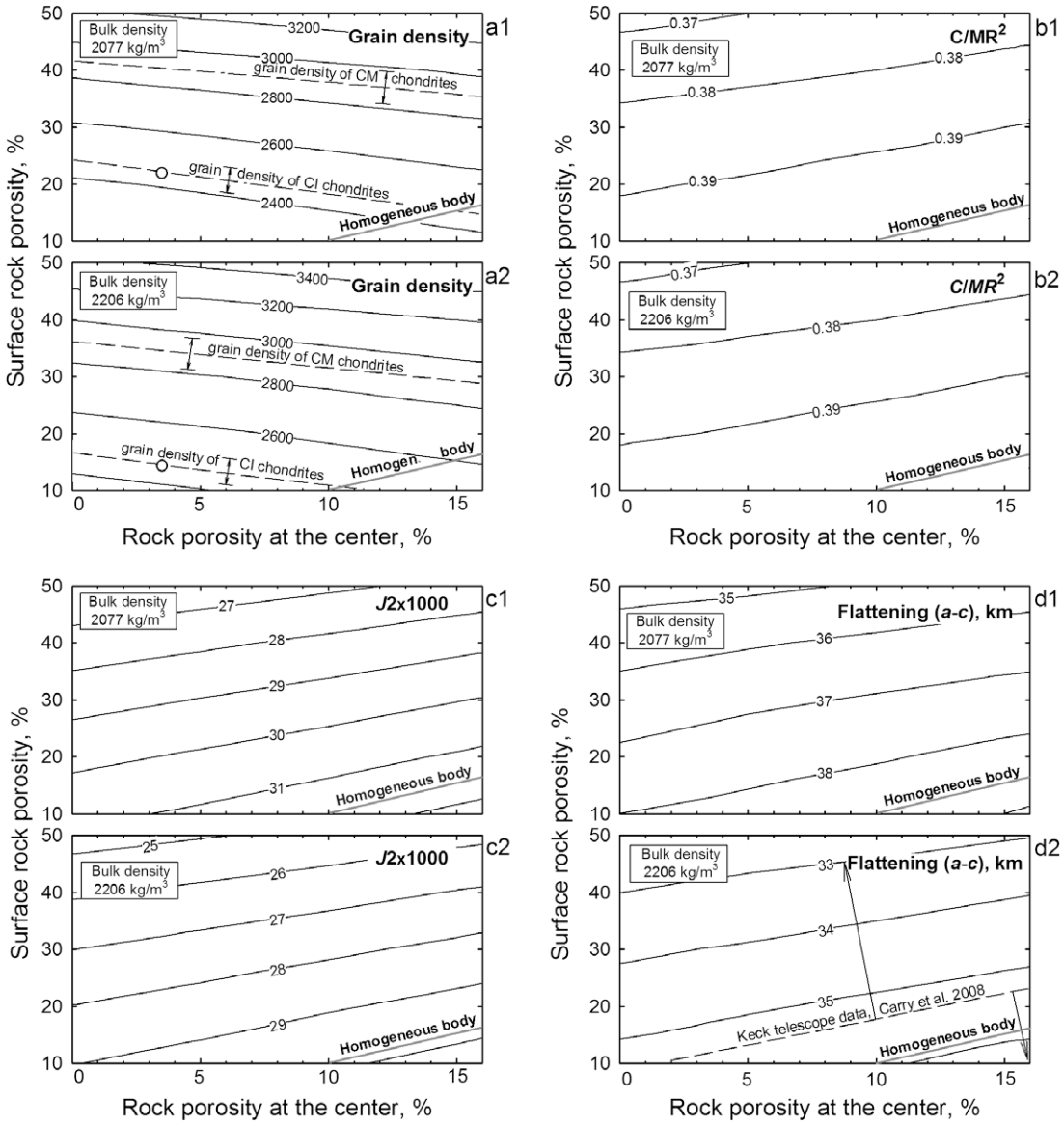

Fig. 3. The modeled grain density (a1,a2), moment of inertia factor (b1,b2), gravitational moment J_2 (c1,c2), and body's flattening (d1,d2) of homogeneous solids distributed according to a porosity gradient in the interior of Ceres. Plots a1, b1, c1 and d1 are for bulk density of 2077 kg m^{-3} (Thomas et al., 2005); a2, b2, c2 and d2 are for bulk density of 2206 kg m^{-3} (Carry et al., 2008). The parameters are calculated as functions of surface rock porosity and porosity at the body's center, assuming a linear porosity change with pressure (see Appendix A). The gray lines represent the homogeneous interior stricture. In (a), dashed lines with error bars show grain densities of CI and CM chondrites from Table 1. The circle open symbols designate example cases shown in Fig. 5. In (d2), the dashed line shows Ceres' flattering with uncertainties from Carry et al. (2008).

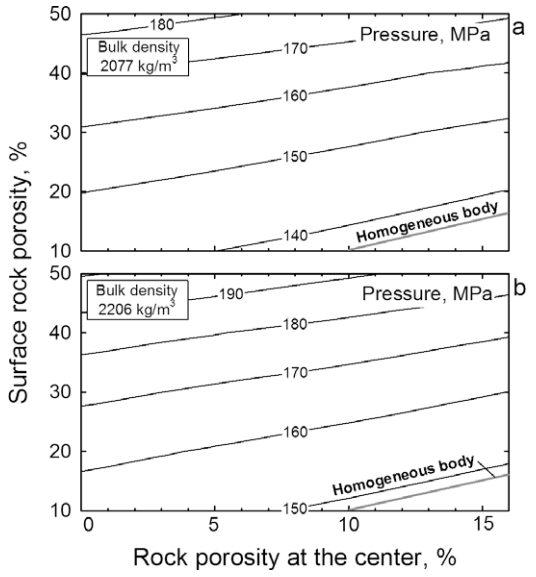

Fig. 4. Pressure in the center part of Ceres. The pressure is calculated with Eq. (A2) in Appendix A. The body consists of homogeneous solids distributed according to a porosity gradient (see caption of Fig. 3). For the model of linear change of porosity with pressure, the central pressure is 170 ± 30 MPa.

characterize a stratified body. Table 2 illustrates that this "collapsed core" model for bulk density 2206 kg m^{-3} leads to polar flattening and J_2 numbers that are similar to these values reported by Carry et al. (2008). For density 2077 kg m^{-3}, calculated flattening and J_2 do not match the values of Thomas et al. (2005). For both bulk densities, evaluated grain density roughly matched that of CI chondrites. Note that compaction pattern and critical pressure of pore collapse remain to be determined for chondritic samples. Until after these data will be available, a gradiental compression approach can be applied for the "compacted center" model.

If compaction of sandstones in sedimentary basins (Allen and Allen, 2005) is used as analogy, surface porosity of 30–40% may decrease linearly to 5–10% porosity in Ceres' center (although exponential change in porosity may occur at $P > \sim 100$ MPa). Here, a linear change of porosity with pressure is used to calculate Ceres' grain density and other physical parameters to satisfy the body's mass and dimensions (see Appendix A for details). Results show that moderately compacted materials with grain densities of CI and CM chondrites can account for the bulk density (Fig. 3a). For example, gradually compacted rocks with the grain density of CI chondrites, 10–20% porosity at the surface and 0–5% porosity in the center agree with the bulk Ceres' density of 2206 kg m^{-3}. Surface porosity of only ~8% higher is needed to be consistent with the bulk density of 2077 kg m^{-3}. In both cases, no additional low-density phases are required if Ceres consists of rocks with grain density similar to that of CI chondrites.

If Ceres consists of solids with the grain density of CM chondrites, significantly higher porosities are required for an ice-free body. For instance, the bulk density of 2206 kg m^{-3} and average porosity of ~24% (Table 1) can be achieved with surface porosity of 35% and center's porosity of 5% (Fig. 3a). At the same center's porosity, the surface porosity of 40% (as in the Tagish Lake chondrite) satisfies the bulk density of 2077 kg m^{-3} and the grain density of CM chondrites. Although Ceres may consist of materials with the grain density of CM chondrites, themselves, these chondrites are not as good rocky analogs as CI chondrites. Results presented in Table 1 and Fig. 3a for the grain density of CM chondrites show that average Ceres' porosity and porosity in upper parts of interior need to be higher than that of typical CM chondrites (~23%). Unavoidable compression of typical CM chondrites in Ceres' interior would require additional low-density phases (e.g., water ice) to be present in the body consisted of CM chondrites.

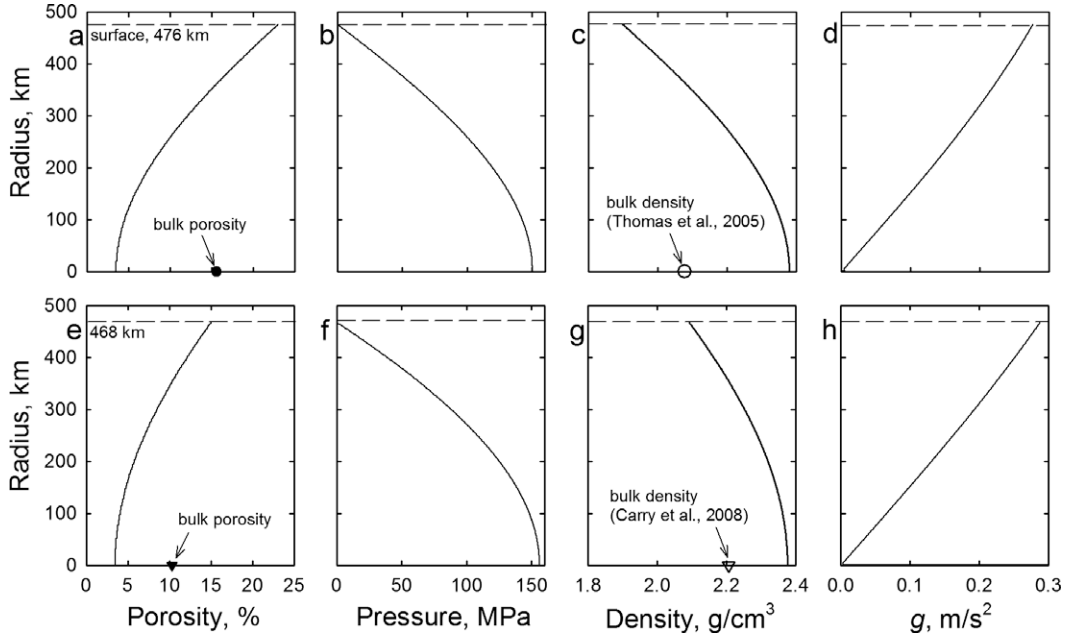

Fig. 5. Physical properties of Ceres' interior with the grain density of CI carbonaceous chondrites (2460 kg m^{-3}, Consolmagno et al., 2008). Profiles of physical properties correspond to bulk density and the equivalent radius ($R = \sqrt[3]{aac}$) from (a–d) Thomas et al. (2005) and (e–h) Carry et al. (2008). The porosity changes linearly with pressure (see Appendix A). In these example calculations, bulk density from Thomas et al. (2005) corresponds to the surface porosity of 23% and the porosity at the center of 3.5%. Data from Carry et al. (2008) match corresponding porosities of 15% and 3.5%. These case porosity values are shown by open circle symbols in Fig. 3a. For (a–d), the calculated moment of inertia factor $C/MR^2 = 0.389$, $J_2 = 29.7 \times 10^{-3}$, geometric oblateness $(a-c)/a = 0.0764$, flattening $(a-c) = 37.2$ km and central $P = 150$ MPa. For (e–h), the corresponding numbers are as follows: 0.393, 28.8×10^{-3}, 0.0733, 35.1 km and 156 MPa.

Moment of inertia dimensionless factors obtained for this "compressed center" model can be as low as ~0.37, and bulk density has no effect on the numbers (Fig. 3b). At strong porosity gradients in ice-free mineralogically uniform Ceres, calculated $J_2 = (25–27) \times 10^{-3}$ (Fig. 3c). These values are higher than J_2 of Thomas et al. (2005) and match J_2 number of Carry et al. (2008) (see Section 1). It follows that body's dimensions and used mass of Thomas et al. (2005) require a more sufficient density gradient than in this model, and may suggest water–rock differentiation. However, data of Carry et al. (2008) can be explained in the framework of the compaction model. This notion is also supported by the comparison of calculated and observed values for polar flattening (Figs. 1 and 3d; Table 2).

Calculated center's pressure for the compaction model vary from ~140 to ~200 MPa (Fig. 4). Larger porosity gradients correspond to higher P. Data reported and used by Thomas et al. (2005) lead to slightly lower P compared to that of Carry et al. (2008).

Fig. 5 shows calculated vertical profiles of physical properties that agree with the grain density of CI chondrites at a specified bulk density and the assumed linear porosity change with P (see Appendix A). Because these conditions can be achieved at different porosities (Fig. 3), center's porosity was chosen arbitrarily in these example calculations. The profiles show that higher porosities and lower densities of surface rocks are needed to satisfy data from Thomas et al. (2005), compared to data from Carry et al. (2008).

4. The nature of Ceres' low-density phases

4.1. Insights from chondrites and comets

Although no known chondrite type fairly matches Ceres' spectra, the body's position in the asteroid belt corresponds to the radial distance where C-class asteroids are most abundant (Gradie et al., 1989). This implies that Ceres can be rich in low-density minerals observed in CI/CM carbonaceous chondrites, and suggested in their parent C-class asteroids (e.g., Jones et al., 1990; Gaffey et al., 2002). As examples, low-density phases can be presented by epsomite (1680 kg m^{-3}), bloedite (2230 kg m^{-3}), saponite (2350 kg m^{-3}), serpentine phases (2440–2800 kg m^{-3}), halite (~2070 kg m^{-3}), tochilinite (2970 kg m^{-3}) and brucite (2390 kg m^{-3}). Most of these minerals are products of aqueous hydration and/or oxidation on parent bodies of many carbonaceous and some ordinary chondrites, and are abundant in CI and/or CM chondrites (Zolensky and McSween, 1988; Brearley and Jones, 1998; Bland et al., 2004; Brearley, 2006). Although brucite is a minor phase in CI chondrites (reported only in Orgueil, Böstrom and Fredriksson, 1966), it could have altered to carbonates in terrestrial conditions (Mumpton and Thompson, 1966). Brucite spectral feature at ~3.06 μm and common formation through aqueous alteration of Earth's ultramafic rocks (serpentinization) make this phase highly suitable for Ceres (Milliken and Rivkin, 2009).

In addition to hydrated and oxidized phases, Ceres could be rich in organic compounds that contribute to the low density. This is consistent with absorption at 3.3–3.4 μm in Ceres' reflectance spectra that may indicate aromatic hydrocarbons (Rivkin et al., 2006; Moroz et al., 1998). Although CI chondrites are rich in carbon, they contain ~10 times less C than the solar photosphere, which represents the Solar System abundance (Palme and Jones, 2003; Asplund et al., 2005). The solar photosphere also contains ~40 times more N than CI chondrites. It follows that outer Solar System bodies could be enriched in C and N compared to known chondrites. This notion is consistent with the data on cometary dust that is rich in "CHON" particles (Jessberger et al., 1988; Fomenkova et al., 1994; Hanner and Bradley, 2005). Even a moderate addition of organic matter to nonporous hydrated rocks with the grain density of CI chondrites leads to values reported for Ceres' bulk density (Fig. 6). A significantly larger amount should be added to CM chondrites to decrease their grain density to the Ceres' values. If an additional organic material is present on Ceres, neither high porosity nor water phases are needed to account for the bulk density. If Ceres represents a captured Kuiper Belt Body (KBO) (McKinnon, 2008), the organic enrichment is likely. However, this excess of organic compounds and Ceres' origin in the outer Solar System are hypothetical and are not required to explain

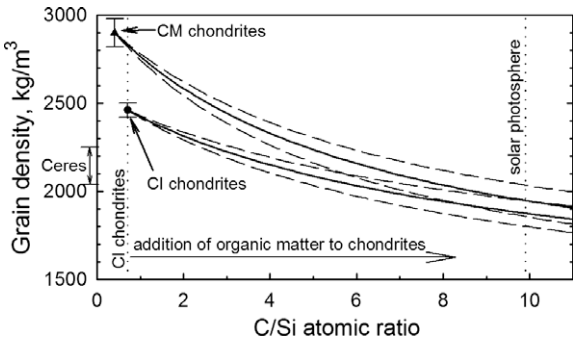

Fig. 6. The effect of addition of organic matter to chondrites on their grain density. The vertical dotted lines represent C/Si atomic ratios in CI chondrites and the solar photosphere from Palme and Jones (2003). The added organic matter corresponds to the composition of insoluble kerogen-like material in the Murchison CM chondrite with 61 atomic% C (Zinner, 1988) and chosen density of 1300 ± 100 kg m^{-3}, which is typical for coal (Johnson and Olhoeft, 1984). The dashed curves show error bars due to the uncertainty in the density of organic matter. Chondrite grain densities are from Consolmagno et al. (2008). The Ceres' data on Y-axes refer to bulk density.

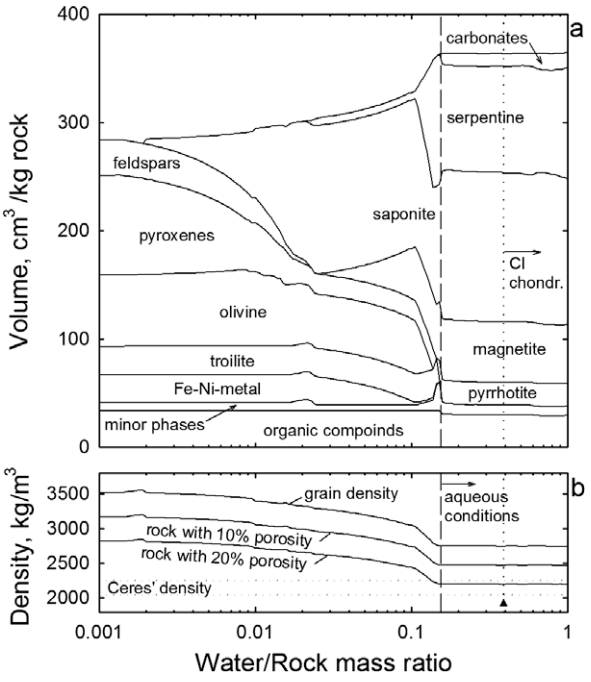

Fig. 7. Modeled volumes of minerals (a) and grain density (b) of aqueously altered CI chondritic material as functions of water/rock ratio. The mineral assemblage represents metastable thermochemical equilibria calculated for 0 °C and 6.1 mbar in closed water–rock system (see Appendix A). The volumes of minerals refer to 1 kg of original rock. The vertical dashed line shows the boundary between anhydrous (metamorphic) and aqueous conditions. The vertical dotted line refers to the lower limit for the W/R ratio for CI chondrites (Clayton and Mayeda, 1999). The horizontal dotted lines show Ceres' bulk density with uncertainties. In panel (b), the triangle symbol corresponds to the grain density of mineral assemblage shown in Table 3.

observations in terms of ice-deficient models for the interior structure.

4.2. Constraints from aqueous alteration models

By analogy with parent asteroids of ordinary and carbonaceous chondrites, Ceres' low-density minerals could have formed through aqueous alteration of initial anhydrous and reduced mineral assemblages formed in the solar nebula. Although aqueous alteration on accreted planetesimals (early formed asteroids) is likely, some later *in situ* aqueous alteration may have occurred as well. If secondary solids have equilibrated with aqueous solution, the phase rule and elemental (bulk) composition of the system would limit the number and amount of the phases. The phase composition should also be affected by the amount of water solution available (i.e. water/rock ratio), temperature, pressure, oxidation–reduction (redox) state, gas escape and duration of the alteration (e.g., Zolensky et al., 1989; Rosenberg et al., 2001; Zolotov et al., 2006). This section presents mineral assemblages obtained through calculations of thermochemical equilibria in water–rock systems, in which bulk rock composition corresponds to CI chondrites (see Appendix A for details).

The calculations demonstrate that bulk grain density of altered chondritic rocks strongly depends on the water/rock (W/R) mass ratio. This is illustrated in Fig. 7, which presents equilibrium mineralogy in closed system in which H_2 has accumulated and sulfides have not been oxidized to sulfates. If $W/R > 0.15$–0.20, the rock could be completely hydrated in the presence of aqueous solution and has grain density of ~2750 kg m^{-3}. Abundant Mg phyllosilicates mainly contribute to the low grain density. Close system models for temperature <350 °C show that at $W/R \sim 0.4$–1, which may represent CI chondrites (Clayton and Mayeda, 1999), the calculated grain density remains ~2700–2800 kg m^{-3}. In this temperature interval, corresponding aqueous solutions are rich in NaCl and do not contain abundant sulfates. Modeled freezing of these solutions led to hydrohalite and significantly smaller amounts of hydrated Na carbonate (natron) and KCl (cf. Zolotov, 2007). Despite a low grain density of these precipitated salts, their amount is limited by the low Na and Cl abundance, and bulk grain density of the rock + salt assemblage is ~2700 kg m^{-3}. The calculated grain densities match that of Orguel CI chondrite (2760 kg m^{-3}, if abundant epsomite and organic matter are not considered, Bland et al., 2004). The modeled densities are only slightly lower than that of CM chondrites (Table 1), which contain some unaltered Mg silicates and cronstedtite with grain density of ~3590 kg m^{-3}. Still, ~20–25% bulk porosity and/or additional low-density phases (ice, organic matter, salt hydrates) are needed for these hydrated but reduced assemblages to account for Ceres' density (Fig. 7b).

Formation of secondary phases with significantly lower densities than that in CM chondrites may require oxidizing aqueous conditions, which are also favored at elevated temperatures. These conditions could have occurred in parent asteroids of CI carbonaceous chondrites. CI chondrites could have been altered at higher temperatures (~150 °C, Clayton and Mayeda, 1999) than CM chondrites and contain ~10 vol.% hydrated sulfates (mostly epsomite, Brearley and Jones, 1998) formed through aqueous oxidation of sulfides. Thermochemical equilibrium evaluations show that sulfates could have formed at elevated temperatures and low H_2 pressures (Zolotov and Shock, 2003). Asteroids with high porosity and permeability could have favored H_2 escape, consistent with higher oxidation state of more porous carbonaceous meteorites (e.g., oxidized CV3 chondrites, Consolmagno et al., 2008). In addition, high temperature significantly increases the oxidation rate of sulfides (Ohmoto and Lasaga, 1982). In addition to hydrothermal conditions and H_2 escape, sulfates could have formed through oxidation of sulfides by H_2O_2 and other oxidants formed through radiolysis of water ice particles before their accretion on planetesimals.

Table 3
Highly hydrated, oxidized and low-density mineral assemblage that may form during thorough aqueous alteration of carbonaceous planetesimals from which Ceres may have accreted.

Mineral/species	Formula	Volume (cm^3) (kg rock)$^{-1}$
Saponite	$Mg_{19}Si_{22}O_{60}(OH)_{12}$	193.0
Epsomite	$MgSO_4{\cdot}7H_2O$	153.0
Hematite	Fe_2O_3	73.3
Mirabilite	$Na_2SO_4{\cdot}10H_2O$	36.0
Pyrene	$C_{16}H_{10}$	32.3
Gypsum	$CaSO_4{\cdot}2H_2O$	16.4
Ni-sulfide	NiS	5.2
Dolomite	$CaMg(CO_3)_2$	3.8
Quartz	SiO_2	3.3
Ca phosphate	$Ca_3(PO_4)_2$	2.2
Hydrohalite	$NaCl{\cdot}2H_2O$	1.6
Minor phases		2.3

Notes: The grain density of this mineral assemblage is ~1910 kg m^{-3}. Minor phases are presented by chromite, serpentine and K sulfate. Pyrene represents high-molecular weight aromatic species. The mineral composition corresponds to the W/R mass ratio of 0.4 (see details in the text and Appendix A).

Modeled assemblages that correspond to oxidizing conditions and involve subsequent freezing (or evaporation) of aqueous solutions, lead to low-density sulfate salts and Mg phyllosilicates. In an end-member case, sulfides could be completely oxidized to sulfates. However, high-molecular weight organic compounds and polymers may have not been oxidized significantly, as observed in carbonaceous chondrites (Sephton, 2002; Alexander et al., 2007). Such a modeled assemblage with bulk grain density of ~1900 kg m^{-3} is shown in Table 3. This grain density is lower than that of CI chondrites because sulfides and some minor primary Mg silicates (Bland et al., 2004) remain in CI chondrites. Overall, these calculations demonstrate that significant oxidation of sulfides and subsequent precipitation of hydrated sulfates cause a significant decrease in bulk grain density. Neither water phases nor high porosity are needed if Ceres' rocks are rich in hydrated sulfates such as epsomite.

5. Formation and fate of Ceres' materials

Pervasively hydrated and oxidized assemblages could have formed on carbonaceous planetesimals before Ceres' accretion. As in carbonaceous chondrites, hydration would have been manifested in the formation of phyllosilicates (serpentine, cronstedtite, saponite, and chlorite) and tochilinite. Oxidation caused formation of magnetite, ferrous silicates, phosphates, chromite, tochilinite, pyrrhotite, pentlandite, sulfates (on some bodies) and carbonates, and affected distribution patterns of trace elements (e.g., Brearley and Jones, 1998; Krot et al., 2000). By analogy with parent asteroids of CI chondrites (Krot et al., 2006), these planetesimals could have altered at least several Myr after the formation of Ca–Al rich inclusions (CAIs) 4567.2 ± 0.6 Myr ago. An earlier formation of these planetesimals would have led to devolatilization of planetesimals due to decay of abundant ^{26}Al. Aqueous processes on carbonaceous planetesimals probably occurred after major ^{26}Al-powered thermal processes in parent bodies of iron and differentiated meteorites (Krot et al., 2006; Scott, 2006). A late formation of carbonaceous planetesimals and/or an elevated amount of accreted water ice led to only a moderate internal heating, partially caused by the exothermic hydration of silicates (Grimm and McSween, 1989). Temperature inside these bodies (<~150 °C, Clayton and Mayeda, 1999) could have been high enough to promote hydration and oxidation, and not high enough to cause dehydration (except for some bodies represented by metamorphosed

CI/CM chondrites). Hydrogen formed through interaction of reduced minerals (e.g., Fe^o metal, phosphides, FeS) and some organic species with water could have escaped from porous planetesimals. Both H_2 escape and elevated temperatures promoted oxidation and sulfate formation (Zolotov and Shock, 2003). A late accretion of Ceres proposed in this paper (at least 7–8 Ma after CAIs) implies thorough aqueous alteration of Ceres-forming planetesimals. By the time of Ceres' accretion, a significant amount of ^{26}Al could have been decayed, rocks hydrated and salts precipitated. Some free water could have been lost through venting and ice sublimation. The carbonaceous planetesimals probably had bulk density and porosity of C-class asteroids (~1400 kg m^{-3}, Standish, 2001; ~20–70%, Britt et al., 2002). Accretion of carbonaceous planetesimals could have led to compaction (i.e. porosity decrease to ~10%) but may not have caused major chemical changes. However, at late stages of accretion and during the late heavy bombardment event ~3.9 Gyr ago (e.g., Gomes et al., 2005) some impact dehydration may have led to mineralogy that is spectrally similar to metamorphosed CM/CI chondrites (cf. Hiroi et al., 1995). These processes may have contributed to unusual spectral features of Ceres' surface.

After Ceres' accretion, mild heating caused by ^{26}Al (if any) and long-lived radionuclides (McCord and Sotin, 2005) may have not caused major dehydration of the interior. A high hydration state of accreted minerals does not imply a contribution of exothermic hydration reactions into heat balance. A saturation of pore space with water vapor (controlled by hydrated minerals or some water phases) and slow diffusion of water vapor toward the surface (Fanale and Salvail, 1989) limited dehydration. In particular, epsomite could have survived because of the high activation energy of dehydration (McCord et al., 2001). Note, however, that low thermal conductivity of hydrated phases and elevated porosity could have favored some dehydration of central Ceres (J. Castillo-Rogez, personal communication). This dehydration should not cause formation of water mantle.

Alternatively, an early formation of Ceres from ^{26}Al-rich planetesimals could have caused devolatilization and may have led to accumulation of salt solutions in peripheral parts of the body (McCord and Sotin, 2005; Castillo-Rogez and McCord, 2009). Rapid rock-water differentiation and a limited H_2 escape should have not favored pervasive rock's hydration and oxidation. Early formed minerals could have been dehydrated leading to higher grain densities, as it have occurred in parent bodies of some CV3 (e.g., Allende, Krot et al., 1998) and metamorphosed CI chondrites (Tonui et al., 2003). This scenario is less consistent with Ceres' density and albedo than a late accretion of altered planetesimals with abundant low-density minerals. A high-temperature processing of Ceres' interior with formation of a dense rocky core is especially inconsistent with the shape and density reported by Carry et al. (2008).

At present, decay of long-lived radionuclides may account for the interior temperature <350–400 K (McCord and Sotin, 2005). (The actual temperature can be different taking into account porosity and a lack of abundant water ice compared to the McCord–Sotin model.) If some water ice has accreted on Ceres, aqueous phase could occupy some pore spaces in a central part of the body. Suggested accretion of pervasively hydrated and oxidized minerals implies that water may have not been consumed in hydration and oxidation reactions in the interior. Earth's rocks become impermeable only at $P > \sim 300$ MPa (Wash and Brace, 1984) and some migration of aqueous solutions is possible in Ceres' interior. Chondrites are permeable (Corrigan et al., 1997) and fluid convection can be possible if the radius of the "aqueous" zone exceeds ~80 km (Travis and Schubert, 2005). Convection of solutions together with diffusion and condensation of water vapor may contribute to the heat transfer toward the surface. Although corresponding mineral dissolution and precipitation would account for specific rock alteration at different radial distances, aqueous solutions cannot exit in an upper part of the interior (McCord and Sotin, 2005; Castillo-Rogez and McCord, 2009) and should not affect surface mineralogy.

A coexistence of rocks with aqueous floods in the central part of Ceres over billions of years would have led to chemical equilibration through acid-base and hydration–dehydration reactions. However, sluggish oxidation–reduction reactions among inorganic and organic species may have not equilibrated. As examples, low-temperature disequilibria among oxidized (sulfates, carbonates) and reduced minerals (Fe^{2+}-oxides, sulfides) and organic matter present in accreted chondritic material may persist over geological time. Likewise, soluble oxidized (sulfate, bicarbonate) and reduced (carboxylic acids, bisulfide, alcohols, urea, etc.) species leached from accreted chondritic material (Brearley and Jones, 1998; Sephton, 2002) do not equilibrate easily at estimated Ceres' temperatures (e.g., Ohmoto and Lasaga, 1982; McCollom and Seewald, 2007). However, rates of these reactions can be accelerated if chemotrophic organisms are present and gain metabolic energy from redox disequilibria. The metabolic reactions may include sulfate reduction, anaerobic oxidation of organic species, ferrous iron oxidation, ferric iron reduction and methanogenesis.

6. Conclusions

1. Ceres' mass and dimensions remain uncertain and do not exclude a slightly differentiated or undifferentiated interior structure. The observed rocky surface may be inconsistent with a large-scale water–rock differentiation. A differentiated structure with a thick water mantle below a rocky crust is gravitationally unstable and an early overturn would have led to abundant surface salt deposits, which are not observed. A formation of hydrated surface minerals through internal heating would require a major devolatilization and increase in bulk density. Aqueous alteration *in situ* is also unlikely at cold low-pressure conditions at the surface. A post-accretion accumulation of a layer of hydrated minerals at the surface is inconsistent with anhydrous surfaces of many asteroids and with the cosmic dust accumulation rates in the inner Solar System. Therefore, the surface material could represent aqueously altered planetesimals from which Ceres accreted.

2. Compressibility data on terrestrial sedimentary rocks together with chondritic data imply that Ceres may preserve ~5–15% porosity. In such a case, there is no need for abundant water phases to be present to account for the bulk density. A compaction-related density gradient in the rocky non-icy interior may account for Ceres' J_2 gravitational moment and polar flattening obtained with Keck telescope by Carry et al. (2008). Gravity experiments with Dawn spacecraft in 2015 would validate J_2 numbers and concerns about a differentiated structure.

3. Ceres may consist of a moderately compacted (~10% porosity) rocky material with grain density of CI carbonaceous chondrites without abundant water ice. Compacted (~10% porosity) analog materials with grain density of CM chondrites imply a presence of water (ice/liquid) and/or other low-density phases. In any case, Ceres probably consists of highly hydrated minerals, but may not contain abundant water ice, at least as a thick interior layer. The mineralogy of CI/CM chondrites and thermochemical equilibrium models for secondary phase composition suggest that phyllosilicates and hydrated salts (especially sulfates) could account for a low grain density of Ceres' rocks. In addition, a high organic content could contribute to the low bulk density. An elevated organic content is likely if Ceres is a captured KBO body. However, the addition of organic matter is not required to explain the data in

terms of hydrated and porous interior structure without abundant ice.

4. The likely low-density hydrated mineralogy of the interior implies Ceres' accretion from pervasively hydrated low-density carbonaceous planetesimals (asteroids) in which ^{26}Al had largely decayed. Abundant water ice may not have accreted. After the accretion (at least 7–8 Ma after the formation CAIs), limited heat sources (McCord and Sotin, 2005) could have not caused major mineral dehydration leading to formation of water mantle.

Acknowledgments

The paper is benefited from review comments and conversations with William McKinnon. The work is supported by Grants from NASA Cosmochemistry Program (NNX07AJ73G) and NASA Astrobiology Institute (NNA09DA79A).

Appendix A. Evaluations of grain density, moment of inertia and J_2

A uniform grain density (ρ_g) is assumed for "compressed center" ice-free models for interior structure. In one set of models (Table 2), porosity (ω) abruptly decreases at a radial distance (r) that corresponds to a specified pressure. In other models (Figs. 3–5), a change of ω with pressure (P) is calculated with linear equation

$$\omega = \omega_s - \left(\frac{\omega_s - \omega_c}{P_c}\right)P, \tag{A1}$$

were ω_s represents porosity of surface rocks, and ω_c and P_c stand for porosity and pressure at the body's center, respectively. At each radial distance, P is calculated by solving equation

$$dP = -g_r \rho_r d_r, \tag{A2}$$

where g_r is the gravitational acceleration, and ρ_r designates bulk rock density at r. The relationship between grain density and bulk rock density is described by Eq. (2) in Section 3.2. The acceleration due to gravity is calculated with

$$g_r = 4/3\pi G\rho r, \tag{A3}$$

where G designates the gravitational constant and ρ denotes bulk density below radial distance r. Eqs. (A1)–(A3) are solved for density to be consisted with reported Ceres' densities.

The moment of inertia C, dimensionless moment of inertia factor (C/MR^2), second degree gravitational moment J_2, geometric oblateness $(a - c)/a$, and flattening $(a - c)$ are calculated with equations

$$C = \frac{8\pi}{3}\int_0^R \rho_r r^4 dr, \tag{A4}$$

$$\frac{C}{MR^2} = \frac{2/3\ J_2}{J_2 + 1/3q_r}, \tag{A5}$$

$$q_r = \frac{W^2R^3}{GM}, \tag{A6}$$

$$\frac{a-c}{a} = \frac{3}{2}J_2 + \frac{q_r}{2}, \tag{A7}$$

where M stands for body's mass, a is semi-major axes and c is minor axes of the ellipsoid, R is the equivalent radius ($\sqrt[3]{aac}$), q_r represents smallness parameter for the rotational distortion, and W designates angular velocity (2π/rotation period). The rotation period is 9.0741 h (Carry et al., 2008). The used equations are after Hussmann (2007), Sohl and Schubert (2007), and de Peter and Lissauer (2001).

The grain density is also calculated for secondary mineral assemblages that could have formed during aqueous alteration on Ceres-forming planetesimals. The assemblages are evaluated through computation of thermochemical equilibria in water–rock systems. The equilibria are calculated for $P = 0.1$ MPa for a range of temperatures and water/rock mass ratios with the modified GEOCHEQ code that considers non-ideal solid, gas and aqueous solutions (Mironenko and Zolotov, 2005). To explore effect of the redox state and potential gas escape, calculations are performed in the system open with respect to H_2. Details of the calculations and data sources can be seen in (Zolotov et al., 2006). Here, the modeled rock is presented by the water-free composition of the Orgueil CI chondrite modified from (Jarosewich, 1990) and Cl abundance for CI chondrites from (Lodders and Fegley, 1998). The composition is as follows, in mole kg^{-1}: O, 17.8409; H, 2.0863; K, 0.0184; Mg, 5.6838; Ca, 0.35; Al, 0.4813; C, 3.3648; Si, 5.4510; P, 0.0447; S, 1.4908; Cr, 0.0592; Na, 0.3540; Cl, 0.0285; Mn, 0.0427; Fe, 4.8704; Co, 0.0122; Ni, 0.2828.

The mineral composition presented in Table 3 is calculated in two steps. First, metastable thermochemical equilibrium is calculated in the open water–rock system at 150 °C, 4.75 bar, W/R mass ratio of 0.4 and H_2 fugacity 10^{-6} bar. The rock composition corresponded to that of Orgueil CI chondrite. Pyrene is a metastable phase, which is used as a proxy for organic species. Then, deposition of salts upon freezing of aqueous solution has modeled with the FREZCHEM code (Marion and Kargel, 2008).

References

Alexander, C.M.O.'D., Fogel, M., Yabuta, H., Cody, G.D., 2007. The origin and evolution of chondrites recorded in the elemental and isotopic compositions of their macromolecular organic matter. Geochim. Cosmichim. Acta 71, 4380–4403.
Allen, P., Allen, J., 2005. Basin Analysis: Principles and Applications. Blackwell Publication, Oxford. pp. 549.
Antonellini, M., Aydin, A., Pollard, D.D., 1994. Microstructure of deformation bands in porous sandstones at Arches National Park. Utah. J. Struct. Geol. 16, 941–959.
Asplund, M., Grevesse, N., Sauval, A.J., 2005. The solar chemical composition. ASP Conf. Ser. 336, 25–38.
Bland, P.A., Cressey, G., Menzies, O.N., 2004. Modal mineralogy of carbonaceous chondrites by X-ray diffraction and Mössbauer spectroscopy. Meteor. Planet. Sci. 39, 3–16.
Böstrom, K., Fredriksson, K., 1966. Surface conditions of the Orgueil meteorite parent body as indicated by mineral associations. Smithsonian Misc. Coll. 151, 1–39.
Brearley, A.J., 2006. Action of water. In: Lauretta, D.S., McSween, H.Y. (Eds.), Meteorites and Early Solar System II. University of Arizona Press, Tucson, pp. 587–624.
Brearley, A.J., Jones, R.H., 1998. Chondritic meteorites. In: Papike, J.J. (Ed.), Planetary Materials, Rev. Mineral. 36. Miner. Soc. Amer, Washington, D.C., pp. 1–398.
Britt, D.T., Yeomans, D., Housen, K., Consolmagno, G., 2002. Asteroid density, porosity, and structure. In: Bottke, W.F., Jr., Cellino, A., Paolicchi, P., Binzel, R.P. (Eds.), Asteroids III. University of Arizona Press, Tucson, pp. 485–500.
Brown, P.G., and 21 colleagues, 2001. The fall, recovery, orbit, and composition of the Tagish Lake meteorite: A new type of carbonaceous chondrite. Science 290, 320–325.
Carry, B., and 7 colleagues, 2008. Near-infrared mapping and physical properties of the dwarf-planet Ceres. Astron. Astrophys. 478, 235–244.
Castillo-Rogez, J.C., McCord, T.B., 2009. Ceres: Evolution and present state constrained by the shape data. Icarus, doi: 10.1016/j.icarus.2009.04.008.
Clayton, R.N., Mayeda, T.K., 1999. Oxygen isotope studies of carbonaceous chondrites. Geochim. Cosmochim. Acta 63, 2089–2104.
Consolmagno, G.J., Britt, D.T., 1998. The density and porosity of meteorites from the Vatican collection. Meteorit. Planet. Sci. 33, 1231–1241.
Consolmagno, G., Britt, D.T., Stoll, C.P., 1998. Metamorphism, shock, and porosity: Why are there meteorites? Meteorit. Planet. Sci. 33 (Suppl.), A34–A35.
Consolmagno, G.J., Britt, D.T., Macke, R.J., 2008. The significance of meteorite density and porosity. Chemie der Erde 68, 1–29.
Corrigan, C.M., and 6 colleagues, 1997. The porosity and permeability of chondritic meteorites and interplanetary dust particles. Meteorit. Planet. Sci. 32, 509–515.
de Peter, I., Lissauer, J.J., 2001. Planetary Sciences. Cambridge University Press. pp. 528.
Dvorkin, J., Mavko, G., Nut, A., 1991. The effect of cementation on the elastic properties of granular materials. Mech. Mat. 12, 207–217.
Edmond, J.M., Paterson, M.S., 1972. Volume change during the deformation of rocks at high pressure. Int. J. Rock Mech. Mining Sci. 9, 161–182.
Fanale, F.P., Salvail, J.R., 1989. The water regime of Asteroid 1 Ceres. Icarus 82, 97–110.
Feierberg, M.A., Lebofsky, L.A., Larson, H.P., 1981. Spectroscopic evidence for aqueous alteration products on the surfaces of low-albedo asteroids. Geochim. Cosmochim. Acta 45, 971–981.
Fomenkova, M.N., Chang, S., Mukhin, L.M., 1994. Carbonaceous components in the Comet Halley dust. Geochim. Cosmochim. Acta 58, 4503–4512.
Gaffey, M.J., Cloutis, E.A., Kelley, M.S., Reed, K.L., 2002. Mineralogy of asteroids. In: Bottke, W.F., Jr., Cellino, A., Paolicchi, P., Binzel, R.P. (Eds.), Asteroids III. University of Arizona Press, Tucson, pp. 183–204.

Giles, M.R., 1997. Diagenesis: A Quantitative Perspective. Implications for Basin Modeling and Rock Property Prediction. Kluwer Academic Publishers. pp. 526.
Gomes, R., Levison, H.F., Tsiganis, K., Morbidelli, A., 2005. Origin of the cataclysmic late heavy bombardment period of the terrestrial planets. Nature 435, 466–469.
Gradie, J., Chapman, C.R., Tedesco, E.F., 1989. Distribution of taxonomic classes and the compositional structure of the asteroid belt. In: Binzel, R.P., Gehrels, T., Matthews, M.S. (Eds.), Asteroids II. University of Arizona Press, Tucson, pp. 316–335.
Grimm, R.E., McSween, H.Y., 1989. Water and the thermal evolution of carbonaceous chondrite parent bodies. Icarus 82, 244–280.
Handin, J., Hatter Jr., R.V., Friedman, M., Feather, J.N., 1963. Experimental deformation of sedimentary rocks under confining pressure: Pore pressure tests. Bull. Am. Ass. Petrol. Geol. 47, 717–755.
Hanner, M.S., Bradley, J.P., 2005. Composition and mineralogy of cometary dust. In: Festou, M.C., Keller, H.U., Weaver, H.A. (Eds.), Comets II. University of Arizona Press, Tucson, pp. 555–564.
Hirata, N., Kurita, K., Sekine, T., 1998. Experimental shock lithification of porous powder mixture. Lunar Planet. Sci. XXXIX. Abstract 1345.
Hiroi, T., Pieters, C.M., Zolensky, M.E., Lipschutz, M.E., 1995. Thermal metamorphism of the C, G, B, and F asteroids seen from the 0.7 μm absorption band in comparison with carbonaceous chondrites. Antarctic Meteorites 20, 72–75.
Hussmann, H., 2007. Interiors and evolution of icy satellites. In: Schubert, G. (Ed.), Treatise on Geophysics, vol. 10. Elsevier, pp. 509–540.
Jarosewich, E., 1990. Chemical analyses of meteorites: A compilation of stony and iron meteorite analyses. Meteoritics 25, 323–337.
Jessberger, E.K., Christoforidis, A., Kissel, J., 1988. Aspects of the major element composition of Halley's dust. Nature 332, 691–695.
Johnson, G.R., Olhoeft, G.R., 1984. Density of rocks and minerals. In: Carmichael, R.S. (Ed.), Handbook of Physical Properties of Rocks, vol. 3. CRC Press, Inc, pp. 2–38.
Jones, T.D., Lebofsky, L.A., Lewis, J.S., Marley, M.S., 1990. The composition and origin of the C, P, and D asteroids: Water as a tracer of thermal evolution in the outer belt. Icarus 88, 172–192.
Kargel, J.S., 1991. Brine volcanism and the interior structures of asteroids and icy satellites. Icarus 94, 368–390.
King, T.V.V., Clark, R.N., Calvin, W.M., Sherman, D.M., Brown, R.H., 1992. Evidence for ammonium-bearing minerals on Ceres. Science 255, 1551–1553.
Kirk, R.L., Stevenson, D.J., 1987. Thermal evolution of a differentiated Ganymede and implications for surface features. Icarus 69, 91–134.
Krot, A.N., Petaev, M.I., Scott, E.R.D., Choi, B-G., Zolensky, M.E., Keil, K., 1998. Progressive alteration in CV3 chondrites: More evidence for asteroidal alteration. Meteorit. Planet. Sci. 33, 1065–1085.
Krot, A.N., Fegley Jr., B., Lodders, K., Palme, H., 2000. Meteoritical and astrophysical constraints on the oxidation states of the solar nebula. In: Mannings, V., Boss, A.P., Russel, S.S. (Eds.), Protostars and Planets IV. University of Arizona Press, Tucson, pp. 1019–1055.
Krot, A.N., Hutcheon, I.D., Brearley, A.J., Pravdivtseva, O.V., Petaev, M.I., Hohenburg, C.M., 2006. Timescales and settings for alteration of chondritic meteorites. In: Lauretta, D.S., McSween, H.Y., Jr. (Eds.), Meteorites and Early Solar System II. University of Arizona Press, Tucson, pp. 525–553.
Lebofsky, L.A., 1978. Asteroid 1 Ceres: Evidence for water of hydration. Mon. Not. Roy. Astron. Soc. 182, 17–21.
Lebofsky, L.A., Feierberg, M.A., Tokunaga, A.T., Larson, H.P., Johnson, J.R., 1981. The 1.7- to 4.2-μ spectrum of Asteroid 1 Ceres – Evidence for structural water in clay minerals. Icarus 48, 453–459.
Li, J-Y., and 7 colleagues, 2006. Photometric analysis of Asteroid 1 Ceres and surface mapping from HST observations. Icarus 182, 143–160.
Lodders, K., Fegley Jr., B., 1998. The Planetary Scientist's Companion. Oxford University Press, New York.
Marion, G.M., Kargel, J.S., 2008. Cold Aqueous Planetary Geochemistry with FREZCHEM: From Modeling to the Search for Life at the Limits. Springer-Verlag, Berlin, Heidelberg. 251 pp.
McCollom, T.M., Seewald, J.S., 2007. Abiotic synthesis of organic compounds in deep-sea hydrothermal environments. Chem. Rev. 107, 382–401.
McCord, T.B., Sotin, C., 2005. Ceres: Evolution and current state. J. Geophys. Res. 110, E05009.
McCord, T.B., and 6 colleagues, 2001. Thermal and radiation stability of the hydrated salt minerals epsomite, mirabilite, and natron under Europa environmental conditions. J. Geophys. Res. 106, 3311–3320.
McKinnon, W.B., 1997. Mystery of Callisto: Is it differentiated? Icarus 130, 540–543.
McKinnon, W.B., 2008. Could Ceres be a refugee from the Kuiper belt? Asteroids, Comets, Meteors 10th. Abstract 8389.
McKinnon, W.B., Parmentier, E.M., 1986. Ganymede and Callisto. In: Burns, J.A., Matthews, M.S. (Eds.), Satellites. University of Arizona Press, Tucson, pp. 718–763.
Menéndez, B., Zhu, W., Wong, T-F., 1996. Micromechanics of brittle faulting and cataclastic flow in Berea sandstone. J. Struct. Geol. 18, 1–16.
Meunier, A., 2005. Clays. Springer, Berlin. 472 pp.
Milliken, R.E., Rivkin, A.S., 2009. Brucite and carbonate assemblages from altered olivine-rich materials on Ceres. Nature Geosci. 2, 258–261.
Mironenko, M.V., Zolotov, M.Yu., 2005. Thermodynamic models for aqueous alteration coupled with volume and pressure changes in asteroids. Lunar Planet. Sci. Conf. XXXVI. Abstract 2207.
Miyamoto, M., Zolensky, M.E., 1992. Infrared diffuse reflectance spectra of carbonaceous chondrites: Amount of hydrated minerals. Proc. ISAS Lunar Planet. Sum. 25th, 32–35.
Miyamoto, M., Jujii, N., Ito, K., Kobayashi, Y., 1982. The fracture strength of meteorites: Its implication for their fragmentation. Met. Natl. Inst. Polar Res. Spec. Issue 25, 331–343.
Moroz, L.V., Arnold, G., Korochantsev, A.V., Wasch, R., 1998. Natural solid bitumens as possible analogs for cometary and asteroid organics. Icarus 134, 253–268.
Mumpton, F.A., Thompson, C.S., 1966. The stability of brucite in the weathering zone of the New Idria serpentinites. Clays Clays Miner. 14, 249–257.
Ohmoto, H., Lasaga, A.C., 1982. Kinetics of reactions between aqueous sulfates and sulfides in hydrothermal systems. Geochim. Cosmochim. Acta 46, 1727–1745.
Palme, H., Jones, A., 2003. Solar System abundances of the elements. In: Holland, H.D., Turekian, K.K. (Eds.), Treatise on Geochemistry, vol. 1. Elsevier, pp. 41–61.
Peucker-Ehrenbrink, B., Schmitz, B. (Eds.), 2001. Accretion of Extraterrestrial Matter Throughout Earth's History. Kluwer Academic/Plenum Publishers, New York e.a., p. 466.
Rappaport, N.J., and 10 colleagues, 2008. The gravity field of Titan from four Cassini flybys. Eos Trans. AGU, (Fall Meet. Suppl.) 89 (52). Abstract P21A-1343.
Rivkin, A.S., Volquardsen, E.L., 2008. Sitting around watching the world Ceres: A rotational study of the innermost dwarf planet. Lunar Planet. Sci. Conf. XXXIX. Abstract 1920.
Rivkin, A.S., Volquardsen, E.L., Clark, B.E., 2006. The surface composition of Ceres: Discovery of carbonates and iron-rich clays. Icarus 185, 563–567.
Rosenberg, N.D., Browning, L., Bourcier, W.L., 2001. Modeling aqueous alteration of CM carbonaceous chondrites. Meteorit. Planet. Sci. 36, 239–244.
Russell, C. T., and 15 colleagues, 2007. Dawn Mission to Vesta and Ceres. Earth Moon Planets 101, 65–91.
Sato, K., Miyamoto, M., Zolensky, M.E., 1997. Absorption bands near 3 μm in diffuse reflectance spectra of carbonaceous chondrites: Comparison with asteroids. Meteorit. Planet. Sci. 32, 503–507.
Schubert, G., Stevenson, D.J., Ellsworth, K., 1981. Internal structures of the Galilean satellites. Icarus 47, 46–59.
Sclater, J.G., Christie, P.A.F., 1980. Continental stretching: An expansion of the post Mid-Cretaceous subsidence of the central North Sea basin. J. Geophys. Res. 85, 3711–3739.
Scott, E.R.D., 2006. Meteoritic and dynamical constraints on the growth mechanisms and formation times of asteroids and Jupiter. Icarus 185, 72–82.
Scott, T.E., Nielsen, K.C., 1991. The effect of porosity on the brittle–ductile transition in sandstones. J. Geophys. Res. 96, 405–414.
Septhon, M.A., 2002. Organic compounds in carbonaceous meteorites. Nat. Prod. Rep. 19, 292–311.
Sohl, F., Schubert, G., 2007. Interior structure, composition and mineralogy of the terrestrial planets. In: Schubert, G. (Ed.), Treatise on Geophysics, vol. 10. Elsevier, pp. 27–68.
Standish, E.M., 2001. JPL Interoffice Memorandum 312.
Strait, M.M., Consolmagno, G., 2004. Variations in microcrack porosity across meteorite types. Meteorit. Planet. Sci. 39 (Suppl.), A100.
Thomas, P.C., and 6 colleagues, 2005. Differentiation of the Asteroid Ceres as revealed by its shape. Nature 437, 224–226.
Tonui, E.K., Zolensky, M.E., Lipschutz, M.E., Wang, M.-S., Nakamura, T., 2003. Yamato-86029: Aqueously altered and thermally metamorphosed CI chondrite with unusual textures. Meteorit. Planet. Sci. 38, 269–292.
Travis, B.J., Schubert, G., 2005. Hydrothermal convection in carbonaceous chondrite parent bodies. Earth Planet. Sci. Lett. 240, 234–250.
Vernazza, P., and 7 colleagues, 2005. Analysis of near-IR spectra of 1 Ceres and 4 Vesta, targets of the Dawn mission. Astron. Astrophys. 436, 1113–1121.
Wash, J.B., Brace, W.F., 1984. The effect of pressure on porosity and the transport properties of rock. J. Geophys. Res. 89, 9425–9432.
Webster, W.J., and 7 colleagues, 1988. The microwave spectrum of Asteroid Ceres. Astron. J. 95, 1263–1268.
Witteborn, F.C., Roush, T.L., Cohen, M., 2000. Thermal emission spectroscopy of 1 Ceres: Evidence for olivine. In: Sitko, M.L., Sprague, A.L., Lynch, D.K. (Eds.), Thermal Emission Spectroscopy and Analysis of Dust, Disks, and Regoliths, Astronom. Soc. of the Pacific Conf. Ser. vol. 196, pp. 197–203.
Wong, T.-F., 1990. Mechanical compaction and the brittle–ductile transition in porous sandstones. In: Knipe, R.J., Rutter, E.H. (Eds.), Deformation Mechanisms, Rheology and Tectonics. Geol. Soc. Spec. Publ. vol. 54, pp. 111–122.
Wong, T.-F., Christian, D., Zhu, W., 1997. The transition from brittle faulting to cataclastic flow in porous sandstones: Mechanical deformation. J. Geophys. Res. 102, 3009–3025.
Yada, T., and 7 colleagues, 2004. The global accretion rate of extraterrestrial materials in the last glacial period estimated from the abundance of micrometeorites in Antarctic glacier ice. Earth Planets Space 56, 67–79.
Yang, Y.L., Aplin, A.C., 2004. Definition and practical application of mudstone porosity–effective stress relationships. Petroleum Geosci. 10, 153–162.
Zinner, E., 1988. Interstellar cloud material in meteorites. In: Kerridge, J., Matthews, M. (Eds.), Meteorites and the Early Solar System. University of Arizona Press, Tucson, pp. 956-983.
Zolensky, M.E., McSween, H.Y., 1988. Aqueous alteration. In: Kerridge, J., Matthews, M. (Eds.), Meteorites and the Early Solar System. University of Arizona Press, Tucson, pp. 114–143.
Zolensky, M.E., Bourcier, W.L., Gooding, J.L., 1989. Aqueous alteration on the hydrous asteroids: Results of EQ3/6 computer simulations. Icarus 78, 411–425.
Zolotov, M.Yu., 2007. An oceanic composition on early and today's Enceladus. Geophys. Res. Lett. 34. DOI:1029/2007GLG031234.L23203.
Zolotov, M.Yu., Shock, E.L., 2003. Aqueous oxidation of parent bodies of carbonaceous chondrites and Galilean satellites driven by hydrogen escape. Lunar Planet. Sci. Conf. XXXIII. Abstract 2047.
Zolotov, M.Yu., Mironenko, M.V., Shock, E.L., 2006. Thermodynamic constraints on fayalite formation on parent bodies of chondrites. Meteorit. Planet. Sci. 41, 1775–1796.